Journal of Chromatography, 149 (1978) 669–682

CHROM. 10,892

POST-COLUMN REACTOR SYSTEMS IN LIQUID CHROMATOGRAPHY

R. S. DEELDER, M. G. F. KROLL and A. J. B. BEEREN
DSM Research, Geleen (The Netherlands)
and
J. H. M. VAN DEN BERG*
Laboratory of Instrumental Analysis, Eindhoven University of Technology, Eindhoven (The Netherlands)

SUMMARY

The sensitivity and selectivity of standard liquid chromatographic detectors such as photometers, fluorimeters and coulometric cells can be substantially improved by coupling the exit of the chromatographic column to a chemical reaction system. The additional band broadening in these reactors should be reduced to an acceptable value by an appropriate design of the system.

Three types of reactors are used: tubular reactors, packed bed reactors and gas-segmented liquid flow systems. The performances and characteristics of these reactor systems are compared and some specific instrumental problems (mixing, noise level) are discussed. Rules for optimal design are given. The choice of the reactor system depends on the speed and the complexity of the reaction involved. This is illustrated by a number of practical applications of both simple, fast reactions and slower reactions that consist of several steps. Results on band broadening in the reactors and on detection limits are given. Some systems are suitable for the determination of sub-nanogram amounts.

INTRODUCTION

Reaction detectors are becoming increasingly important as a means of for improving the sensitivity and selectivity for specific applications of column liquid chromatography. In the simplest design, a suitable reagent specific for the group of compounds to be determined is added continuously to the column effluent and the coloured reaction products formed are detected photometrically. The ninhydrin system for amino acids is an example of this group of reaction colorimeters, and was among the first detectors to be used extensively on a routine basis in column liquid chromatography. However, post-column reactors can also be used in combination with fluorimetry[1–5] or electrochemical detection[6].

As discussed elsewhere[7–9], the basic problem with reaction detectors is the additional broadening of the chromatographic peaks that occurs in these systems. Let the variance, expressed in time units, of a solute band leaving the column be $\Delta\sigma_{tc}^2$, the variance of the residence time distribution function in the reaction detector

* Present address: DSM Research, Geleen, The Netherlands.

$\Delta\sigma_{tr}^2$ and the final variance of the peak as observed in the detector σ_t^2. The variances are additive, and therefore

$$\sigma_t^2 = \Delta\sigma_{tc}^2 + \Delta\sigma_{tr}^2 \tag{1}$$

In a properly designed reaction system, the additional band broadening should be as low as possible in order to reduce the adverse effect on resolution.

THEORETICAL: REACTOR TYPES

Tubular reactors

In their simplest form, flow reactors consist of narrow tubing. In straight, open tubes with laminar flow, a residence time distribution orginates from the combination of the parabolic velocity profile and molecular diffusion. If it is accepted that the variance $\Delta\sigma_{tr}^2$ in such a reactor tube can be approximated by the variance of the residence time distribution function of an inert, non-reacting compound, the following equation can be used[10]:

$$\Delta\sigma_{tr}^2 = \frac{2D_m t_v^3}{L^2} + \frac{d_t^2 t_v}{96 D_m} \tag{2}$$

where t_v is the mean residence time, L the length of the reactor tube and D_m the molecular diffusion coefficient of the tracer compound. This equation can be used only if $\Delta\sigma_{tr} \ll t_v$, $Ld_t/(t_v D_m) > 100$ and $t_v D_m/d_t^2 > 0.2$ (ref. 11). Except for extremely low and impractical flow velocities, the first term on the right-hand side of eqn. 2 can be neglected, giving

$$\frac{\Delta\sigma_{tr}^2}{t_v} = \frac{d_t^2}{96 D_m} \tag{3}$$

For a non-parabolic flow profile, this equation can be modified to

$$\frac{\Delta\sigma_{tr}^2}{t_v} = \frac{\kappa d_t^2}{96 D_m} \tag{4}$$

where κ depends on the particular flow profile[12].

When a fluid flows through a helically coiled tube, a secondary flow that is perpendicular to the main direction of flow sets in (Fig. 1). This secondary flow is due to centrifugal forces acting on the moving fluid. Axial velocity is greatest near the centre of the tube, and here centrifugal forces will act most strongly. The fluid near the centre is thrown outwards and is continuously replaced with fluid recirculating along the tube wall. The first theoretical study of flow in curved tubes was made by Dean[13], who obtained an approximate expression for the fluid velocity profile by solving analytically the equations of motion. He proposed the use of a dimensionless parameter, known as the Dean number, $Dn = Re\sqrt{d_t/d_c}$, for characterizing flow in curved tubes, where Re is the Reynolds number and $Re = 4\varrho\Phi/\pi d_t\eta$, ϱ the density of the solvent, η the viscosity of the solvent, Φ the volumetric flow-rate, d_t the tube diameter and d_c the coil diameter. Owing to simplifications made in the mathematical procedures, Dean's solutions are valid only for a very limited range of flow conditions.

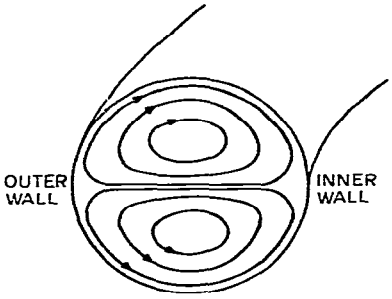

Fig. 1. Secondary flow pattern in the cross-section of a coiled tube.

More recently, numerical methods have been used[14,15] for solving the equations of motion over a wide range of Reynolds numbers and curvature ratios, $\lambda = d_c/d_t$.

The calculated axial flow velocity profiles were found to deviate strongly from their parabolic straight-tube counterparts; the differences between the mean axial velocity and the velocity of the various axial streamlines are greatly reduced. These results were confirmed experimentally[15]. Secondary flow in coiled tubes causes an increase in radial mass transfer and therefore reduces axial dispersion in comparison with flow through a straight tube.

Horváth *et al.*[16] attempted to exploit this phenomenon in liquid chromatography and investigated band broadening in coiled, uncoated capillary columns. Experimentally, a considerable decrease in band broadening due to the "coiling effect" was observed. The residual dispersion, however, was still unacceptable for liquid chromatography.

From the point of view of fluid mechanics, the problem of dispersion in the laminar flow of an incompressible fluid in curved channels consists essentially in solving the mass-transfer equation, accounting for both molecular and convective diffusion in a given flow field. Because of the complexity of the equations involved, no satisfactory solution for this problem has been found up to now.

Recently, Trivedi and Vasudeva[17] presented experimental results for dispersion in coiled tubes over a wide range of Dean numbers; they found that plotting the experimental κ values against Dn gave a series of curves according to the Schmidt number, Sc, where $Sc = \eta\varrho/D_m$. However, as at least some of the κ values were calculated incorrectly from asymmetrical step response curves, the reliability of the results is doubtful. A recent theoretical study[18,19] showed that κ can be calculated as a function of Dn^2Sc for $d_c/d_t > 20$ and $Dn < 15$, but no experimental verification has been presented.

We therefore measured κ values for three solute–solvent pairs in tubes of length 10–20 m and I.D. 0.5–1.0 mm for various curvature ratios, λ (ref. 20). In Fig. 2 the κ values are plotted against $DnSc^{\frac{1}{2}}$. The data points are represented by a single curve, as predicted by Janssen[18,19]. The following expressions were used to correlate the data:

$$\begin{aligned} \kappa &= 5.6\,(DnSc^{0.5})^{-0.67} \quad \text{for} \quad 12.5 < DnSc^{0.5} < 200 \\ \kappa &= 1 \qquad\qquad\qquad\quad \text{for} \quad DnSc^{0.5} \leqslant 12.5. \end{aligned} \tag{5}$$

The full lines in Fig. 2 correspond to these equations. By using these correlations,

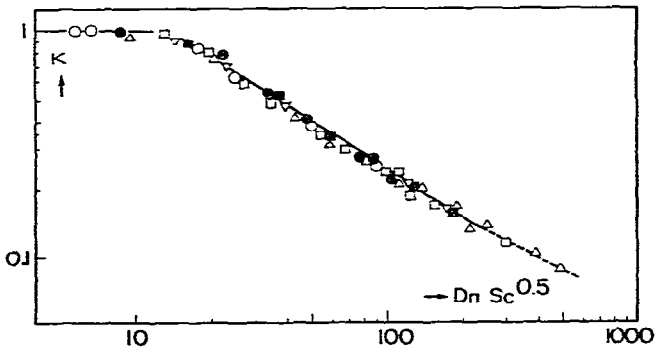

Fig. 2. Reduction of axial dispersion due to secondary flow in coiled tubes; κ values were calculated from experimental data by using eqn. 4 (ref. 20). Open symbols, nitrobenzene–isooctane: ○, λ = 1024; ▽, λ = 305; □, λ = 155; △, λ = 55. ■, Benzene–chloroform, λ = 305. ●, Benzene–hexane, λ = 1024.

it is possible to predict band broadening in coiled tubular reactor systems. In Fig. 3, $\Delta\sigma_{tr}$ is plotted against the internal diameter, d_t, of the reactor tube for various reaction times, t_v. The curves were calculated from eqn. 4 with $\Phi = 1\ \mathrm{cm^3 \cdot min^{-1}}$, $\lambda = 200$, $D_m = 2 \cdot 10^{-5}\ \mathrm{cm^2 \cdot sec^{-1}}$, $\eta = 0.5$ cP and $\varrho = 0.7\ \mathrm{g \cdot cm^{-3}}$.

The pressure drop for laminar flow through straight tubes is calculated from the Poiseuille equation:

$$\frac{\Delta p}{t_v} = \frac{512\,\eta\,\Phi^2}{\pi^2\,d_t^6} \tag{6}$$

Secondary flow in coiled tubes causes an increase in the axial pressure gradient. Considerable experimental data on pressure drop in coiled tubes are available[21,22]

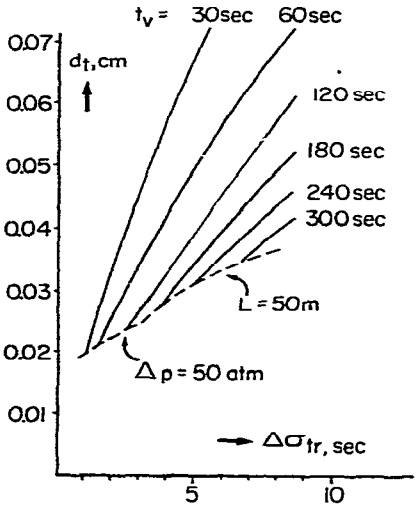

Fig. 3. Band broadening in coiled tubular reactors as a function of the tube diameter, d_t, for various reaction times, t_v.

and a good theoretical background for the empirical pressure drop relationships has been given[15]. It turns out that for $Dn < 25$ the increase in pressure drop is no more than 10% compared with flow through a straight tube. As in practice this condition will always be fulfilled for post-column reactors, eqn. 6 can be used as a good approximation for calculating the pressure drop in these reactors.

It can be seen from Fig. 3 that little additonal band broadening will be obtained for narrow-bore tubes. At a given residence time in the reactor, t_v, the minimal inside diameter of the reactor tube, d_t, will be limited for practical reasons by the pressure drop and tube length. Arbitrarily, a pressure limit of 50 atm and a maximal length of 50 m were chosen. For the various reaction times, t_v, indicated in Fig. 3, the minimal value of d_t was calculated from eqn. 6. On the other hand, a limiting value for d_t was calculated for a tube length of 50 m from:

$$d_t = \left(\frac{4\,\Phi\,t_v}{\pi\,L}\right)^{1/2} \tag{7}$$

The limits of d_t are indicated in Fig. 3.

Packed reactors

Band broadening in columns packed with inert, impervious particles such as glass beads is due to a combination of axial molecular diffusion and convective mixing and can be expressed through the following empirical relationship according to Hiby[23]:

$$H = \frac{L\Delta\,\sigma_{tr}^2}{t_v^2} = \frac{2\,\gamma\,D_m}{u} + \frac{\lambda_1\,d_p}{1 + \lambda_2\left(\frac{D_m}{u d_p}\right)^{1/2}} \tag{8}$$

where γ is the tortuosity factor, u the interstitial fluid velocity, d_p the mean particle size of the packing material and λ_1 and λ_2 are constants characterizing the geometry of the packed bed. The contribution of convective mixing, expressed in the second term on the right-hand side of eqn. 8, can be reduced considerably by using appropriate column packing techniques, and plate heights corresponding to 1–2 times d_p are then obtained[20,24]. This finding suggests that columns packed with small glass beads can be useful as post-column reactors[7].

The variance of the residence time distribution in the reactor, $\Delta\sigma_{tr}^2$, should meet the requirements of the chromatographic column concerned. A suitable choice should therefore be made of the reactor length, L, and particle size of the glass beads, d_p, for a given combination of reaction time, t_v, and additional band broadening, $\Delta\sigma_{tr}$. In practice, limits are set to the pressure drop over the reactor, Δp, and the reactor length, L. The pressure drop is calculated from the Darcy equation:

$$\Delta p = \frac{u\,\eta\,L}{k_0\,d_p^2} \tag{9}$$

where k_0 is the permeability constant of the reactor. Combination of eqns. 8 and 9 gives

$$\xi^{3/2} - \psi\,\xi^{1/2} - \psi\,\frac{\lambda_2}{L}\,(D_m\,t_v)^{1/2} = 0 \tag{10}$$

where

$$\xi = \left(\frac{\eta}{k_0\, t_v\, \Delta p}\right)^{1/2} \tag{11}$$

and

$$\psi = \frac{1}{\lambda_1}\left(\frac{\Delta\, \sigma_{tv}{}^2}{t_v{}^2} - \frac{2\gamma\, D_m\, t_v}{L^2}\right) \tag{12}$$

When $\Delta\sigma_{tr}$ and t_v are fixed, Δp can be calculated from eqn. 10 for any value of L (ref. 7). The corresponding value of d_p is then calculated from eqn. 9. These calculations were carried out for $\gamma = 0.7$, $D_m = 2\cdot 10^{-5}$ cm$^2\cdot$sec^{-1}, $\lambda_1 = 10$, $\lambda_2 = 18$, $k_0 = 2\cdot 10^{-3}$ and $\eta = 0.5$ cP. The values of the Hiby constants λ_1 and λ_2 and the permeability constant k_0 were determined in separate experiments with glass-bead columns[20]; the values of the diffusion coefficient and the viscosity correspond to those used in the preceding section.

In Fig. 4, d_p is plotted against $\Delta\sigma_{tr}$ for various reaction times, t_v, and for $L = 30$ cm. The broken lines interconnect points of equal pressure drop, Δp, over the reactor. For a given length of the reactor, the inside diameter, d_r, should be chosen so as to agree with the reaction time and the volumetric flow-rate through the reactor:

$$d_t = \left[\frac{4t_v\,(\Phi_c + \Phi_r)}{\eta\, \varepsilon_r\, L}\right]^{1/2} \tag{13}$$

where Φ_c and Φ_r denote the column effluent flow-rate and the reagent flow-rate, respectively, and ε_r is the void fraction of the reactor.

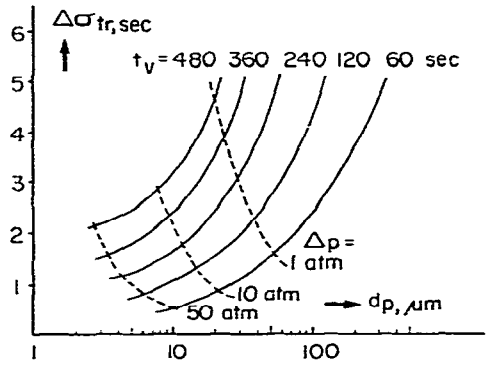

Fig. 4. Band broadening in packed bed reactors as a function of the particle diameter, d_t, for various reaction times, t_v, and for a reactor length of 30 cm.

Segmented flow reactors

Axial dispersion in open-tubular reactors can be considerably reduced by using gas-segmented liquid flow. This type of reactor is widely used in automated colorimetric analysers such as the Technicon AutoAnalyzer systems. In these reactors, the column effluent is fed into a continuous series of short slugs of reagent separated

by air bubbles. Leakage between the segments of the reaction mixture is brought about by fluid from a segment wetting the wall of the reactor tube and mixing with the next segment[25].

Mixing in the acceptor slug is due mainly to the circulating flow within each segment[26–28]. Prediction of the axial dispersion resulting from this mechanism is possible only if the leakage flow and mixing within the slugs can be accurately described. To our knowledge, no rigorous theoretical treatment of this problem has been reported.

Recently, Snyder[8] gave the following semi-empirical expression for the dispersion in segmented-flow reactors:

$$\Delta\sigma_{tr}^2 = \left[\frac{0.14\, d_t^{2/3}\,(\Phi + nV_G)^{5/3}\,\eta^{2/3}}{\sigma^{2/3}\, D_R\, \Phi} + \frac{1}{n}\right]\cdot\left[\frac{2.35\,(\Phi + n\,V_G)^{5/3}\,\eta^{\,2/3} t_v}{\sigma^{2/3}\,\Phi\, d_t^{4/3}}\right] \quad (14)$$

where d_t is the inside diameter of the reactor tube, Φ the liquid flow-rate through the reactor, n the segmention frequency *i.e.* the number of air bubbles injected per unit time, V_G the volume of a gas bubble, η the viscosity of the reaction mixture, and σ its surface tension.

Mixing in the fluid slugs is represented by a flow with a flat velocity profile equal to the actual mean velocity of the slug and with a radial dispersion coefficient, D_R, which accounts for the enhanced mass transfer[12]. Moreover, the thickness of the liquid slug left behind by the fluid slug is calculated by using a well known equation from fluid mechanics[29,30]. In fact, D_R depends on the actual flow pattern in the slug, and

$$D_R = D_R\,(Re,\, Sc,\, \beta,\, \lambda,\, \ldots.)$$

where $\beta = l/d_t$, the dimensionless slug length, l is the actual slug length and $\lambda = d_c/d_t$, the curvature ratio.

However, in eqn. 14, D_R is assumed to have a constant value and Snyder and Adler[31] calculated a mean value of D_R from an extensive series of experimental $\Delta\sigma_{tr}^2$ values using this equation. The measurements were carried out for a single tracer substance and for $Sc \approx 2500$, $10 < Re < 100$ and $10 < \beta < 200$. In these ranges, variations in the radial mass transfer rate are probably limited[28].

In practice, the values of Φ, η, σ, t_v and D_R are fixed by the chromatographic separation and the reaction involved. Now, $\Delta\sigma_{tr}$ can be minimized by a proper choice of the tube diameter, d_t, and the slug frequency, n. In Fig. 5, $\Delta\sigma_{tr}$ is plotted against n for different tube diameters and for a reaction time $t_v = 60$ sec. The other relevant parameters were chosen as in the preceding sections, *i.e.*, $\Phi = 1.0\ \mathrm{cm^3 \cdot min^{-1}}$, $\eta = 0.5$ cP and $D_R = 5 \cdot 10^{-5}\ \mathrm{cm^2 \cdot sec^{-1}}$, the last value being estimated for $D_m = 2 \cdot 10^{-5}\ \mathrm{cm^2 \cdot sec^{-1}}$ as outlined by Snyder[8]. Further, $\sigma = 25\ \mathrm{dyne \cdot cm^{-1}}$; for V_G the minimum air bubble was taken, *i.e.*, $V_G = 0.92\, d_t^3$ (refs. 8 and 32).

Considering that in normal equipment for segmented-flow reactions the slug frequencies do not exceed $2\ \mathrm{sec^{-1}}$, we can see from Fig. 5 that the minimal values attainable in practice do not differ significantly. The choice of the tube diameter, d_t, is therefore not critical here. In Fig. 6, $\Delta\sigma_{tr}$ is plotted against the tube diameter, d_t, for various reaction times, t_v, at the optimal slug frequency or at $n = 2$ if the optimal frequency was found at $n > 2$.

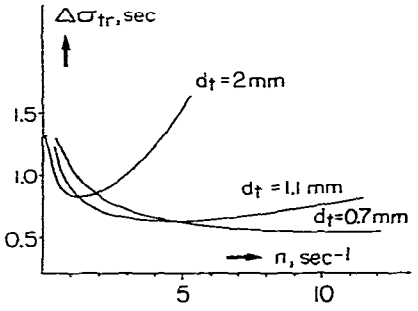

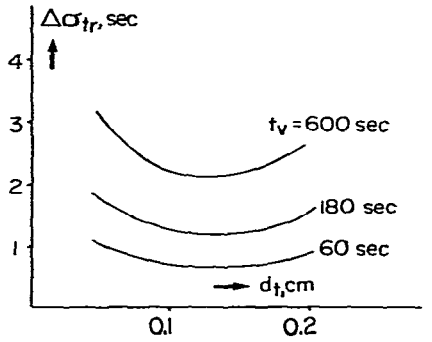

Fig. 5. Band broadening in gas-segmented flow reactors as a function of the segmentation rate, n, for various tube diameters, d_t.

Fig. 6. Band broadening in gas-segmented flow reactors as a function of the tube diameter, d_t, for various reaction times, t_v, at optimized values of the segmentation rate.

Eqn. 14 only expresses band broadening from the reaction coil itself. Practical experience with gas-segmented flow reactors in liquid chromatography shows that mixing tees, connectors and debubblers contribute significantly to the overall dispersion in the reactor system[9,33]. In particular the debubbler seems to have an adverse effect at this point as liquid hold-up is needed in order to prevent air bubbles from being sucked into the flow cell. Fig. 7 shows the dispersion in a combination of a mixing tee and a debubbler. The measurements were carried out as described earlier[9] for 2-mm I.D. tubing. The flow in the system was varied and the volumes of the liquid and air bubbles were kept constant at 0.04 and 0.02 cm^3, respectively. The additional broadening particularly affects the performance of the reactors for short residence times, *e.g.*, 1–5 min. To make the most of the theoretical performance of segmented-flow reactors, the conventional debubblers should be eliminated. Systems that permit photometric measurements on air-segmented liquid flow by means of

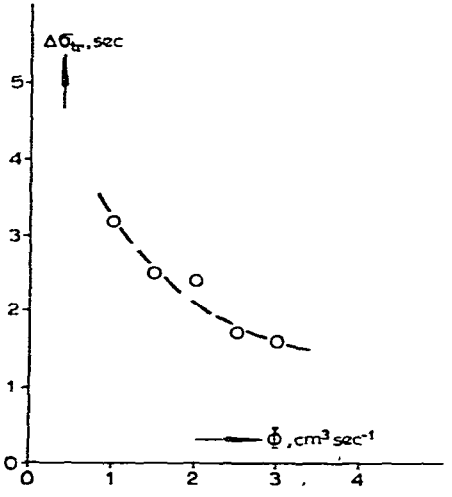

Fig. 7. Band broadening as a function of flow-rate, Φ, for a mixing-tee debubbler combination.

so-called electronic debubbling[34] are used in highly automated clinical analysers; these systems are not yet commercially available for use in liquid chromatography.

EXPERIMENTAL AND RESULTS

Where practical applications of reactor systems are concerned, the "chemistry" of the reaction involved is of the utmost importance for the choice of the reactor type. For simple, one-step fast reactions this choice is straightforward. As demonstrated in the preceding section, the lowest additional band broadening is obtained for packed reactors, *i.e.* $\Delta\sigma_{tr} \leqslant 1$ sec for reaction times up to 3–4 min. A comparable performance cannot be obtained for the other reactor types and packed reactors are, therefore, to be preferred. We have reported earlier on the use of a packed reactor in a colorimetric detection system for hydroperoxides[7].

Fig. 8 gives the scheme of a reaction system for the fluorimetric detection of amino acids separated by "soap chromatography"[35]; the reaction with *o*-phthalaldehyde was used[2]. The reagent was prepared from a Fluescin® solution (Merck, Darmstadt, G.F.R.) according to the manufacturer's instructions. Oxygen-free solutions were used throughout. The linear velocity of the eluent in the chromatographic column corresponds to a volume flow-rate of 1 $cm^3 \cdot min^{-1}$. The flow-rate of the reagent was set arbitrarely at the same value. Mixing of the column effluent and reagent was achieved by using a tee in which both streams were fed through 0.15-mm I.D. channels. This construction ensures a maximal impulse exchange, which favours rapid mixing. The completeness of mixing was verified experimentally by using indicator techniques[36,37]. At 20°, the reaction was almost complete for $t_v = 60$ sec. The reaction was carried out in a 30 cm × 4.6 mm stainless-steel reactor packed with 15-μm glass beads[7]. It can be calculated from eqn. 13 that, for $\Phi_c + \Phi_r = 2$ $cm^3 \cdot min^{-1}$, the mean residence time in the reactor will be about 60 sec. Further, as can be seen from Fig. 4, this reaction can be carried out for $\Delta\sigma_{tr} \approx 1$ sec at a moderate pressure drop.

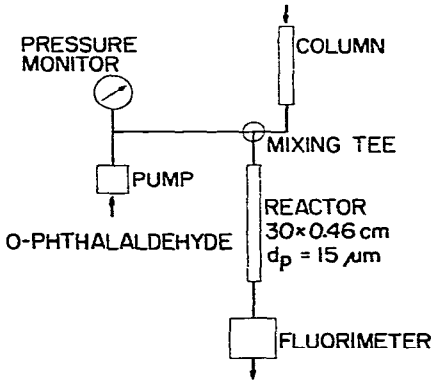

Fig. 8. Schematic diagram of the system for the separation and fluorimetric detection of amino acids.

The fluorescence of the reaction mixture was measured continuously at 445 mm (GG 435 filter) with an FS 970 fluorimeter (Schoeffel Instrument Corp., Westwood, N.J., U.S.A.); the excitation wavelength was 340 nm and the detector time constant was 0.3 sec. Fig. 9 shows a chromatogram of a mixture of amino acids, each peak

corresponding to 1 ng. As can be seen, the minimal detectable amount of the amino acids will be about 100 pg or less, even for strongly retained compounds. It should be emphasized that these detection limits are attained only when fluctuations in the column and reagent flow-rates are virtually eliminated. Reciprocating high-pressure pumps (DMPSK 15, Orlita, Giessen, G.F.R.) equipped with an effective pulse-damping circuit were used.

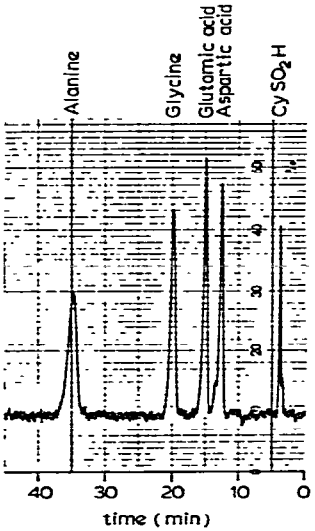

Fig. 9. Chromatogram of a mixture of amino acids. Column: 10 cm × 0.46 cm I.D., packed with 5-μm LiChrosorb RP 8. Eluent, 0.01 *M* phosphate buffer (pH 2.25) in water + 1% *n*-propanol + 0.05% sodium laurylsulphate. Flow-rates: eluent, 1.0 $cm^3 \cdot min^{-1}$; reagent, 1.0 $cm^3 \cdot min^{-1}$. Column and reactor temperature: 25°.

The additional band broadening in the reaction system, $\Delta\sigma_{tr}$, was measured experimentally. For this purpose, a UV-absorbing amino acid, tyrosine, was injected into the chromatographic column, which had been connected directly to a UV detector (PM 2 D, Zeiss, Oberkochen, G.F.R.). The eluent had been modified by adding methanol in order to reduce the capacity factor for tyrosine to about 1. The reactor was then placed between the column and the detector; the reagent flow was replaced by water. The same compound was injected again and $\Delta\sigma_{tr}$ was calculated by comparing the widths of the peaks; a value of about 1 sec was found.

Helically coiled tubes are attractive as reactors, because of their simple construction and the easily predictable dispersion. However, in spite of the "coiling effect", the dispersion in these reactors is relatively important: even for fast reactions ($t_v = 30$ sec), the additional band broadening, $\Delta\sigma_{tr}$, will be about 1 sec (see Fig. 3) and packed reactors are to be preferred. In some applications the properties of the reagent are such as to preclude the use of reactors packed with glass beads. Recently, Takata and Muto[6] described a method for detecting reducing sugars by combination of a reaction system and electrochemical detection:

$$\text{Reducing sugar} + Fe(CN)_6^{3-} \rightarrow Fe(CN)_6^{4-}$$
$$Fe(CN)_6^{4-} \rightarrow Fe(CN)_6^{3-} + e$$

The reaction occurs in alkaline solution at high temperature ($t_v = 2$ min at 90°). Glass-bead columns cannot be used for this reaction as alkaline solutions attack the packing material.

For this reaction we used a tubular reactor. The scheme of the reaction system is shown in Fig. 10. Sugars were separated on a strongly acidic cation-exchange resin (Aminex A-9; Bio-Rad Labs., Richmond, Calif., U.S.A.) in the K^+ form[38]. Deionized water was used as the eluent at a flow-rate of 0.35 $cm^3 \cdot min^{-1}$. The column effluent was mixed with the reagent, consisting of a solution of 0.01 *M* potassium hexacyanoferrate(III) in 0.3 *M* sodium hydroxide solution, flow-rate 0.3 $cm^3 \cdot min^{-1}$. A coiled 316 stainless-steel capillary tube (25 m × 0.254 mm I.D.) was used as a reactor; the coil diameter was 2.5 cm. A coulometric detector as described by Lankelma and Poppe[39] was used for measuring the concentration of the reduced ion $Fe(CN)_6^{4-}$. The particular reaction mixture made it necessary for the detector to be slightly modified. The glassy carbon electrodes were replaced with platinum sheets, and an external calomel electrode was used instead of the internal reference electrode. The working electrode had a constant potential of +0.5 V. Fig. 11 shows a chromatogram of a mixture of sugars. The additional band broadening in the reaction system was 5 sec and the pressure drop was 18 atm. The band broadening was measured by injecting fructose directly into the reactor.

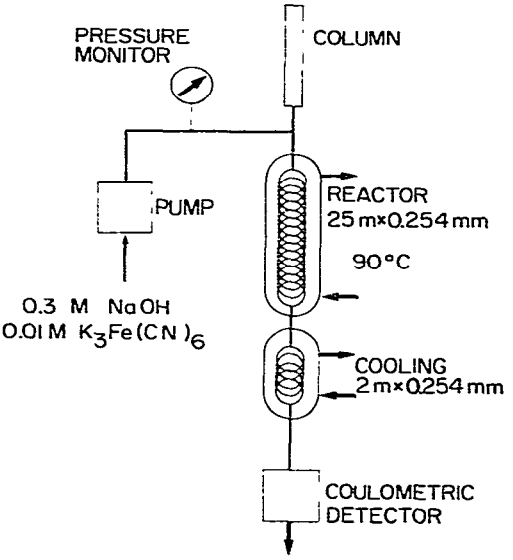

Fig. 10. Schematic diagram of the system for the separation and detection of reducing sugars.

For slow reactions, neither glass-bead columns nor helically coiled reactors can be used without accepting large values for the additional band broadening, $\Delta\sigma_{rr}$. It should be noted, however, that many reputedly slow reactions can be considerably accelerated as the closed pressurized reactor allows the reaction mixture to be heated to temperatures that exceed the boiling point of the solvent[40]. For some applications, however, this approach is unsuitable, *e.g.*, when aggressive reagents such as concentrated acids are used.

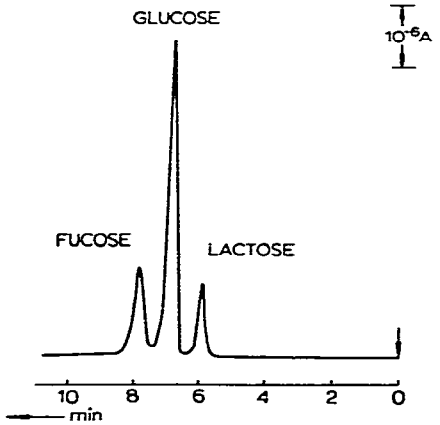

Fig. 11. Chromatogram of a mixture of sugars. Column: 25 × 0.46 cm I.D., packed with Aminex A-9 (K^+) cation-exchanger. Eluent: water. Flow-rates: eluent, 0.35 $cm^3 \cdot min^{-1}$; reagent, 0.3 $cm^3 \cdot min^{-1}$. The fucose peak corresponds to 1.6 μg.

Fig. 12 shows the reaction system used in our laboratory for detecting condensed phosphates used as stabilizers in liquid fertilizers[41]. The separation was carried out on a strongly basic anion-exchange resin (DA-X 8, Durrum, Palo Alto, Calif., U.S.A.) and by using a single-step gradient of sodium chloride (0.25 to 0.4 *M*) in an acetate buffer of pH 4.5 (0.2 *M*). Sulphuric acid (5 *N*) at a flow-rate of 1.0 $cm^3 \cdot min^{-1}$ was added to the column effluent (0.33 $cm^3 \cdot min^{-1}$) and the condensed phosphates hydrolyzed to orthophosphate (the uncondensed form). For tripolyphosphate:

$$P_3O_{10}^{5-} + H_2O \rightarrow P_2O_7^{4-} + PO_4^{3-} + 2H^+$$
$$P_2O_7^{4-} + H_2O \rightarrow 2PO_4^{3-} + 2H^+$$

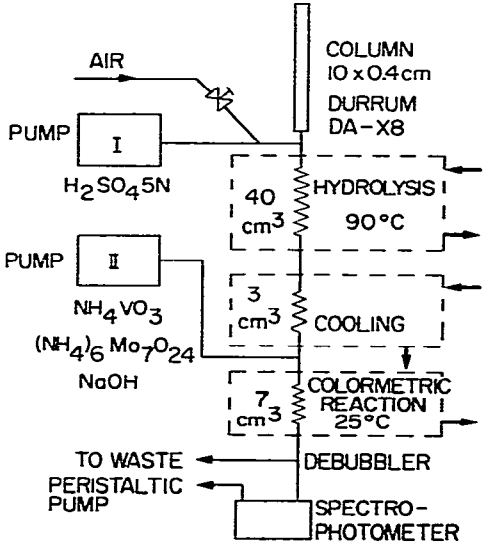

Fig. 12. Schematic diagram of the system for the separation and detection of condensed phosphates.

The hydrolysis was carried out in a segmented flow reactor at 90°; 2-mm I.D. glass tubing was used throughout.

The residence time in the hydrolysis section was about 8 min. The orthophosphate formed was detected by the well known phosphovanadomolybdate colorimetric method[42]. A yellow colour is formed when orthophosphate vanadate and molybdate react in acidic solution; the optimal colour development occurred at pH ≈ 1. Sodium hydroxide was added to the vanadomolybdate reagent to reduce the acidity of the reaction mixture. Colour development was complete in 2 min. The absorbance of the reaction mixture was measured continuously at 420 nm with a PM 2 D spectrophotometer (Zeiss).

Various pumping systems were used for the reaction system. Rather noisy detector signals were found with peristaltic pumps (10^{-3} absorbance units peak-to-peak or worse). In the preferred arrangement, a double-head all-PTFE/KEL-F piston pump (PMP-Duo, Ismatec, Zürich, Switzerland) was used for adding the reagents.

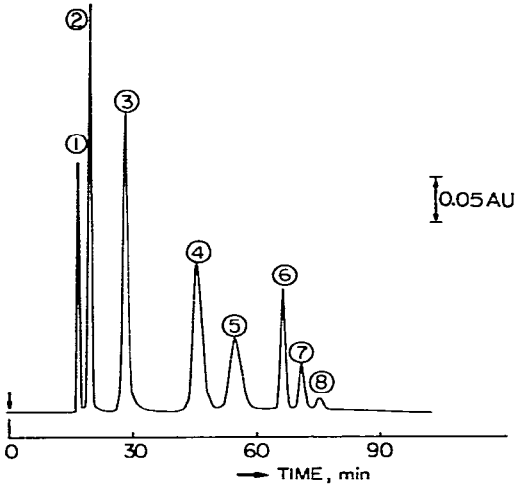

Fig. 13. Chromatogram of a mixture of phosphates. Column: 10 cm × 4 mm I.D., packed with Durrum DA-X 8 anion exchanger. Eluent: sodium chloride (gradient) in acetate buffer (pH 4.5) (see text); flow-rate, 0.33 $cm^3 \cdot min^{-1}$. Peaks: 1 = orthophosphate; 2 = pyrophosphate; 3 = tripolyphosphate; 4 = tetrapolyphosphate; 5 = pentapolyphosphate; 6 = hexapolyphosphate; 7 = heptapolyphosphate; 8 = octapolyphosphate.

TABLE I

CONTRIBUTION OF THE VARIOUS PARTS OF THE REACTOR SYSTEM FOR CONDENSED PHOSPHATES TO $\Delta\sigma_{tr}^2$

Component of reactor system	$\Delta\sigma_{tr}^2$ *(sec²)*	*Residence time (min)*
Hydrolysis and cooling section	39	10
Colour reaction	2	2
Mixing tees and debubbler	8	
Total dispersion	49	12

The segmentation air was added through a capillary bubble-generating system[28]. A noise level of $2–5 \cdot 10^{-4}$ absorbance units was found for this arrangement.

Fig. 13 shows a chromatogram for a mixture of phosphates. The contributions of the various parts of the detection system to the overall variance, σ_{tr}^2, were determined by injecting a suitable tracer, peroxodisulphatotitanic acid, $H_2[TiO_2(SO_4)_2]$, into the reactor. The component in question was removed from the system and the decrease in variance was determined. The results are given in Table I.

REFERENCES

1 S. Udenfried, S. Stein, P. Bohlen, W. Dairman, W. Leingruber and M. Weigele, *Science*, 178 (1972) 871.
2 M. Roth and A. Hampaï, *J. Chromatogr.*, 83 (1973) 353.
3 S. Katz and W. W. Pitt, Jr., *Anal. Lett.*, 5 (1972) 177.
4 Sj. van der Wal and J. F. K. Huber, *J. Chromatogr.*, 135 (1977) 305.
5 R. G. Muusze and J. F. K. Huber, *J. Chromatogr. Sci.*, 12 (1974) 779.
6 Y. Takata and G. Muto, *Anal. Chem.*, 45 (1973) 1864.
7 R. S. Deelder, M. G. F. Kroll and J. H. M. van den Berg, *J Chromatogr.*, 125 (1976) 307.
8 L. R. Snyder, *J. Chromatogr.*, 125 (1976) 287.
9 R. S. Deelder and P. J. H. Hendricks, *J. Chromatogr.*, 83 (1973) 343.
10 R. A. Aris, *Proc. Roy. Soc. London*, A 235 (1956) 67.
11 V. Ananthakrishnan, W. N. Gill and A. J. Barduhn, *AIChE J.*, 11 (1965) 1063.
12 K. B. Bischoff and O. Levenspiel, *Chem. Eng. Sci.*, 17 (1962) 245 and 257.
13 W. R. Dean, *Phil. Mag.*, 4 (1927) 208; 5 (1928) 673.
14 L. C. Truesdell, Jr. and R. J. Adler, *AIChE J.*, 16 (1970) 1010.
15 L. R. Austin and J. D. Seader, *AIChE J.*, 19 (1973) 85.
16 C. G. Horváth, B. A. Preiss and S. R. Lipsky, *Anal. Chem.*, 39 (1967) 1422.
17 R. N. Trivedi and K. Vasudeva, *Chem. Eng. Sci.*, 29 (1974) 2291; 30 (1975) 317
18 L. A. M. Janssen, *Chem. Eng. Sci.*, 31 (1976) 215.
19 L. A. M. Janssen, *Thesis*, University of Technology, Delft, 1977.
20 J. H. M. van den Berg, *Thesis*, University of Technology, Eindhoven, 1978.
21 C. M. White, *Proc. Roy. Soc. London*, A 123 (1929) 645.
22 J. Larrain and C. F. Bonilla, *Trans. Soc. Rheol.*, 14 (1970) 135.
23 J. W. Hiby, in P. A. Rottenburg (Editor), Proceedings of Symposium on *Interaction Between Fluids and Particles*, Institution of Chemical Engineers, London, 1962, p. 312.
24 J. N. Done and J. H. Knox, *J. Chromatogr. Sci.*, 10 (1972) 606.
25 G. Ertingshausen, H. J. Adler and A. S. Reichler, *J. Chromatogr.*, 42 (1969) 355.
26 D. R. Oliver and S. J. Wright, *Brit. Chem. Eng.*, 9 (1964) 590.
27 J. L. Duda and J. S. Vrentas, *J. Fluid. Mech.*, 45 (1971) 247.
28 C. Horváth, B. A. Solomon and J. M. Engasser, *Ind. Chem. Eng. Fundam.*, 12 (1973) 431.
29 L. D. Landau and V. G. Levich, *Acta Phys. Chim. USSR*, 17 (1942) 41.
30 P. Concus, *J. Phys. Chem.*, 74 (1970) 1818.
31 L. R. Snyder and H. J. Adler, *Anal. Chem.*, 48 (1976) 1017 and 1022.
32 F. Fairbrother and A. E. Stubbs, *J. Chem. Soc.*, (1935) 527.
33 G. M. Singer, S. S. Singer and D. G. Schmidt, *J. Chromatogr.*, 133 (1977) 59.
34 R. L. Habig, B. W. Schlein, L. Walters and R. E. Thiers, *Clin. Chem.*, 15 (1969) 1045.
35 J. H. Knox and G. R. Laird, *J. Chromatogr.*, 122 (1976) 17.
36 P. V. Danckwerts, *Chem. Eng. Sci.*, 7 (1957) 116.
37 K. K. Hartung and J. W. Hiby, *Chem.-Ing.-Tech.*, 44 (1972) 1051.
38 R. W. Goulding, *J. Chromatogr.*, 103 (1975) 229.
39 J. Lankelma and H. Poppe, *J. Chromatogr.*, 125 (1976) 375.
40 K. Jonker, *Thesis*, University of Amsterdam, 1977.
41 R. S. Deelder and A. J. B. Beeren, *Anal. Chim. Acta*, submitted for publication.
42 I. M. Kolthoff, P. J. Elving and E. B. Sandell, *Treatise on Analytical Chemistry, Part II*, Vol. 5, Interscience, New York, 1961, p. 351.